© 2021. Published by The Company of Biologists Ltd | Development (2021) 148, dev198028. doi:10.1242/dev.198028

RESEARCH ARTICLE

Stem integrity in *Arabidopsis thaliana* requires a load-bearing epidermis

Mariko Asaoka[1,2,*], Mao Ooe[1,*], Shizuka Gunji[1,3], Pascale Milani[4], Gaël Runel[4], Gorou Horiguchi[5,6], Olivier Hamant[2,7], Shinichiro Sawa[8], Hirokazu Tsukaya[9] and Ali Ferjani[1,3,‡]

ABSTRACT

Because plant cells are glued to each other via their cell walls, failure to coordinate growth among adjacent cells can create cracks in tissues. Here, we find that the unbalanced growth of inner and outer tissues in the *clavata3 de-etiolated3* (*clv3 det3*) mutant of *Arabidopsis thaliana* stretched epidermal cells, ultimately generating cracks in stems. Stem growth slowed before cracks appeared along *clv3 det3* stems, whereas inner pith cells became drastically distorted and accelerated their growth, yielding to stress, after the appearance of cracks. This is consistent with a key role of the epidermis in restricting growth. Mechanical property measurements recorded using an atomic force microscope revealed that epidermal cell wall stiffness decreased in *det3* and *clv3 det3* epidermises. Thus, we hypothesized that stem integrity depends on the epidermal resistance to mechanical stress. To formally test this hypothesis, we used the *DET3* gene as part of a tissue-specific strategy to complement cell expansion defects. Epidermis-driven DET3 expression restored growth and restored the frequency of stem cracking to 20% of the *clv3 det3* mutant, demonstrating the DET3-dependent load-bearing role of the epidermis.

KEY WORDS: *Arabidopsis thaliana*, *clv3 det3* mutant, Mechanical confliction, Stem cracking, Epidermis, Cell wall stiffness

INTRODUCTION

Growth coordination among cells and tissues within a plant organ is considered crucial for the shape and integrity of plant structures. Biochemical cues, such as hormones and microRNA gradients, contribute to such supracellular coordination (Finet and Jaillais, 2012; Skopelitis et al., 2017). Because cells within plant tissues are glued together via their walls, collective growth generates significant mechanical stress (Sassi and Traas, 2015). Such stress can act as an additional cue to coordinate growth. For example, supracellular alignment of cortical microtubules guides cellulose deposition and reinforces epidermal cell walls, enabling them to withstand tensile stress in plant stems (Verger et al., 2018). Two major questions arise: What is the nature of the interplay between biochemical and biomechanical signaling? What is the relative contribution of inner and outer tissues in coordinating growth (both mechanically and biochemically)?

In our previous study, we reported that *Arabidopsis thaliana clv3-8 det3-1* double mutants, with molecular lesions in both *CLAVATA3* (*CLV3*) and *DE-ETIOLATED 3* (*DET3*) genes, exhibit deep longitudinal cracks within their inflorescence stems (Maeda et al., 2014). The CLV3 peptide signal is perceived directly by CLV1 and CLV2, suppressing *WUSCHEL* expression (Miwa et al., 2008, 2009; Müller et al., 2008; Betsuyaku et al., 2011; Kinoshita et al., 2010). In the absence of *CLV3*, the central zone of the shoot apical meristem is enlarged owing to a delay in transition to the peripheral zone in which new organs are generated (Laufs et al., 1998). Together with a long-distance impact on cell proliferation (Reddy and Meyerowitz, 2005), possibly through a scaling mechanism involving a geometrical feedback (Gruel et al., 2016), this enlarged central zone promotes the development of thicker stems. *DET3* encodes subunit C of vacuolar H^+-ATPase and is ubiquitously expressed in both roots and shoots throughout the plant life cycle. Vacuolar ATPases are often abundantly expressed in cells involved in active vesicular trafficking and secretion, and several vacuolar ATPase mutants exhibit growth defects (Padmanaban et al., 2004). These vacuolar ATPase mutants may show reductions in cell-wall stiffness and in ATPase activity. In this respect, *DET3* is an essential gene, as a complete loss of function results in lethality (Schumacher et al., 1999). A knockdown allele, *det3-1*, has been generated. It bears a point mutation (T→A) 32 bp upstream of the putative 3′ splice site junction, and the mutant still holds ∼50% of mRNA, protein and V-ATPase activity (Schumacher et al., 1999; Fukao et al., 2011). *DET3* is particularly important for lignin and carbohydrate biosynthesis, as well as for proton transmembrane transport (Schumacher et al., 1999; Caño-Delgado et al., 2000; Newman et al., 2004; Rogers et al., 2005). The *det3-1* mutant exhibits reduced levels of cellulose synthesis due to impaired secretion and recycling of the cellulose synthase complexes to the plasma membrane (Caño-Delgado et al., 2003; Luo et al., 2015). We hypothesized that the cracked stem phenotype in *cvl3-8 det3-1* results from excessive growth driven by the *clv3-8* mutation and weaker mechanical properties resulting from the *det3-1* mutation. Here, we tested this hypothesis through growth analysis, mechanical assessments and genetic complementation.

From a biophysical perspective, the inflorescence stem is often considered a ‘pressurized vessel’ (Kutschera and Niklas, 2007; Baskin and Jensen, 2013; Hamant and Haswell, 2017). Stem structure is classically viewed as a two-component system, with the outermost component, the epidermis, under tension and the remaining inner components under compression (Hejnowicz and Sievers, 1996; Niklas and Paolillo, 1997). The balance between tension and compression implies that the epidermis is a load-bearing layer,

[1]Department of Biology, Tokyo Gakugei University, 184-8501 Tokyo, Japan. [2]Laboratoire de Reproduction et Développement des Plantes, Université de Lyon, ENS de Lyon, UCB Lyon 1, CNRS, INRAE, 69007 Lyon, France. [3]United Graduated School of Education, Tokyo Gakugei University, 184-8501 Tokyo, Japan. [4]BioMeca company, Ecole Normale Superieure de Lyon, 69007 Lyon, France. [5]Department of Life Science, College of Science, Rikkyo University, 171-0021 Tokyo, Japan. [6]Research Center for Life Science, College of Science, Rikkyo University, 171-0021 Tokyo, Japan. [7]The International Research Organization for Advanced Science and Technology, Kumamoto University, 860-8555 Kumamoto, Japan. [8]Graduate School of Science and Technology, Kumamoto University, 860-8555 Kumamoto, Japan. [9]Department of Biological Sciences, Graduate School of Science, The University of Tokyo, 113-0033 Tokyo, Japan.
*These authors contributed equally to this work

‡Author for correspondence (ferjani@u-gakugei.ac.jp)

H.T., 0000-0002-4430-4538; A.F., 0000-0003-1157-3261

Handling Editor: Ykä Helariutta
Received 23 October 2020; Accepted 11 January 2021

Development (2021) 148, dev198028. doi:10.1242/dev.198028

whereas the inner tissue is held in place by the epidermis (Peters and Tomos, 2000; Galletti et al., 2016). For a cylindrical structure such as a stem, tensile stress is predicted to be twice as high in the transverse direction as in the longitudinal direction. This is consistent with the longitudinal gaping wounds that appear after incisions (Kutschera and Niklas, 2007) and in cell–cell adhesion mutants (Verger et al., 2018). More generally, this is also consistent with the observation that dwarf mutant phenotypes can be complemented by expressing the wild-type (WT) gene in the epidermis (Savaldi-Goldstein et al., 2007; Vaseva et al., 2018). Therefore, spontaneous longitudinal cracking of *clv3-8 det3-1* mutant stems may also be due to high transverse tensile stress in the epidermis. However, this remains debated. In roots, the endodermis, rather than the epidermis, is generally considered the load-bearing layer (Vermeer et al., 2014). Furthermore, tensile stress direction throughout inner tissues plays an important role in generating flat leaves, whereas the cellular response to stress in the epidermis would have to be inhibited for flat leaves to form (Zhao et al., 2020). Here, we have studied the *clv3 det3* double mutant because it provides a unique opportunity to test the epidermal growth theory in a context where wounds are not induced mechanically or genetically but emerge solely as a result of growth.

RESULTS

Altered pith cell differentiation in *clv det3* mutants correlates with cracks

In previous work, we found a correlation between the extent of cell proliferation and stem cracking frequencies in the *det3-1* mutant background, with *clv1* and *clv2* exhibiting the weakest phenotypes and *clv3* the strongest. Indeed, the frequency of cracks in *clv1-4 det3-1* and *clv2-1 det3-1* stems were 37% and 35%, respectively, significantly less than that in *clv3-8 det3-1* stems, in which the cracking frequency was almost 100% (Maeda et al., 2014). To gain further insight into this correlation, we prepared histological cross-sections of inflorescence stems, quantified their cellular parameters and investigated whether there was a correlation between the frequency of stem cracks and inner tissue phenotypes (Fig. 1). Tissue cross-sections showed that the pith cells in all the mutants in the *det3-1* background were distorted, as we reported previously for *det3-1* and *clv3-8 det3-1* (Maeda et al., 2014), although the pith cell morphological defects were relatively mild in *clv2-1 det3-1* (Fig. 1A). Stem section perimeter measurements correlated positively with the number of vascular bundles (R^2=0.57; Fig. 1B). Similarly, cross-sectional areas correlated positively with epidermal cell numbers (R^2=0.88; Fig. 1C). These results indicate that *clv* mutations independently enhance stem thickening and increase the number of epidermal cells and vascular bundles, even in the *det3-1* mutant background. However, there was little correlation between pith cell numbers and cross-sectional areas (R^2=0.08; Fig. 1D), reflecting an excessive increase in pith cell numbers relative to stem thickening. Importantly, *clv3-8 det3-1* stems contained approximately twice as many pith cells as WT stems, despite their similar stem cross-sectional areas (Fig. 1D). Taken together, these results indicate that an excessive increase in the number of stem inner-tissue cells occurs in all *clv det3-1* mutants. However, the low correlation between pith cell

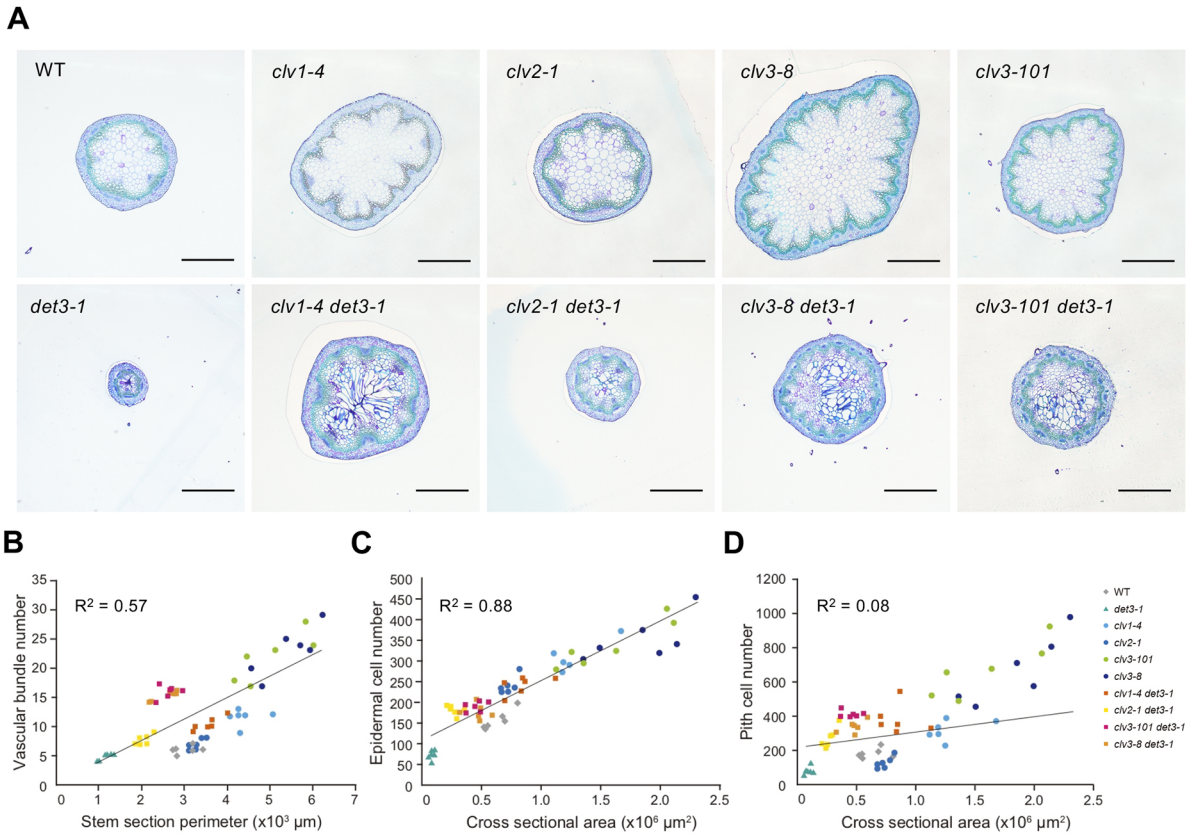

Fig. 1. Quantitative comparative analyses of the inner stem morphology of cracked mutants. (A) Histological cross-sections showing inner tissue organization of inflorescence stems of all genotypes used in this study. Plants were grown for 40 days after sowing before their stems were collected and fixed for histological analyses. Images show a representative cross-section from a stem of each genotype. Histological sections were stained with Toluidine Blue. Scale bars: 500 µm. (B-D) Correlations among stem anatomy parameters. The cross-sectional area, stem section perimeter, number of epidermal cells (C), number of pith cells (D) and number of vascular bundles (B) in the stem inflorescence were quantified using histological images (*n*=6 stems).

Development (2021) 148, dev198028. doi:10.1242/dev.198028

numbers and stem thickness suggests that pith cell features may also be a secondary effect of the mutations. In other words, altered cell differentiation may be triggered by both the *det3-1* mutation and in response to cracks in the stem.

The *det3-1* mutation limits stem growth, whereas pith cell distortion is enhanced after stem cracking

We used kinetic analyses to disentangle the different contributions of the *clv3* and *det3* mutations to stem cracks, growth and pith cell differentiation. First, we focused on the temporal relationship between stem cracks and growth. Compared with WT plants, stem axial growth in the *clv3-8 det3-1* mutant was slow, and this became obvious three days after bolting (Fig. 2A,B). Interestingly, the *det3-1* mutant exhibited the same stem growth defects as *clv3-8 det3-1*, whereas *clv3-8* exhibited an almost normal growth pattern (Fig. 2A,B). Therefore, the *det3* mutation is epistatic to *clv3*.

Next, we monitored the timing of crack occurrence on a daily basis (Fig. 2C). Our time course analyses revealed that cracks in the stem occurred most frequently when *clv3-8 det3-1* stems were ∼2 cm long, and all plants examined had cracks before their stems reached 3 cm in length (Fig. 2C). We also noticed that stem elongation varied among individual plants: stem elongation was either slow or totally arrested after bolting. Nevertheless, even in relatively short stems, the first cracks appeared at later stages. Together, these results show that slow inflorescence stem growth precedes nascent cracks in the *clv3-8 det3-1* mutant. This suggests that cracks are a secondary effect of growth, which is consistent with the epidermis resisting and limiting growth before it yields and cracks.

Next, we analyzed the temporal relationship between stem cracks and pith cell differentiation. To do so, we analyzed pith cell differentiation relative to the size and age of cracks in *clv3-8 det3-1* stems. Our previous work showed that the stem cracks extend longitudinally. Therefore, cracks that appear early can be distinguished from those that appear later (Maeda et al., 2014). Longitudinal sections of the *clv3-8 det3-1* stem showed that pith cells exhibited random shapes and growth directions (Fig. 3A). Whereas pith cells in WT plants were typically piled up in columns, those in *clv3-8 det3-1* were transversely arranged in distorted shapes (Fig. 3A). Although deformed pith cells appeared to be spread across the entire stem, a series of cross-sections revealed that pith cells were not distorted before stem cracking (Fig. 3B). In contrast, pith cells were severely distorted at crack sites, further suggesting that altered differentiation is also a consequence of stem cracking (Fig. 3B).

Next, we prepared cross-sections on the day that a crack occurred from two different parts of the same inflorescence stem: at the cracked region (basal part) and uncracked region (upper part). Pith cells from the upper part of the stem generally showed mild deformation, whereas those from the crack sites were severely distorted (Fig. S1). Note that cracks consistently occurred at interfascicular regions and never through vascular bundles, probably because the former are mechanically weak (Fig. 3).

To confirm these results, we compared stem morphology at four key growth stages, which were selected based on inflorescence stem length. Stem portions were dissected at 5 mm from the base when the main inflorescence stems reached 1, 2, 3 or 4 cm in length, and histological cross-sections were prepared (Fig. 4, Fig. S2). We found that pith cells in the 1- and 2-cm stems of *det3-1* and *clv3-8 det3*-1 mutants were round, whereas those in stems that were at least 3 cm in length exhibited severely distorted shapes (Fig. 4). Furthermore, ultraviolet illumination revealed ectopic lignification in *det3-1* mutants after pith cells were deformed, whereas in WT plants, lignification was restricted to the xylem (Fig. S3). Therefore, we concluded that, although pith cell distortion basically correlates with stem aging, it is further enhanced following the cracks in *clv3-8 det3-1* mutant stems.

A feedback loop between cracks and growth

Based on the observations described above, stem cracks may slow growth further by promoting pith cell lignification or increase growth by freeing the inner tissues from a mechanically resistant outer layer. To test these scenarios, we compared real and theoretical cross-sectional areas, calculated from stem section perimeter measurements. To estimate the theoretical cross-sectional area, we assume that stem cross-section is circular. Therefore, ratios between

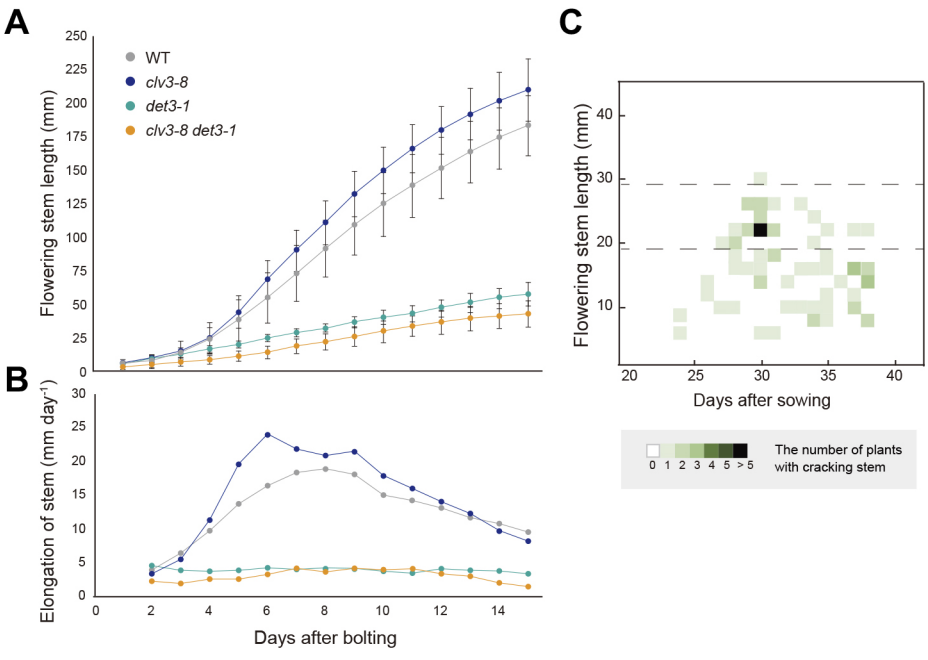

Fig. 2. Correlation between stem growth and the time when cracks occurred. (A,B) Length (A) and elongation rate (B) of flowering stems were recorded for 15 days after stems emerged. Data are mean±s.d. (*n*=16 stems). (C) Plant age (*x*-axis) was plotted against main flowering stem length (*y*-axis) for every first cracking event identified in *clv3-8 det3-1* (*n*=79 stems). A color code indicates the number of plants in which the first crack was identified at each time point.

Development (2021) 148, dev198028. doi:10.1242/dev.198028

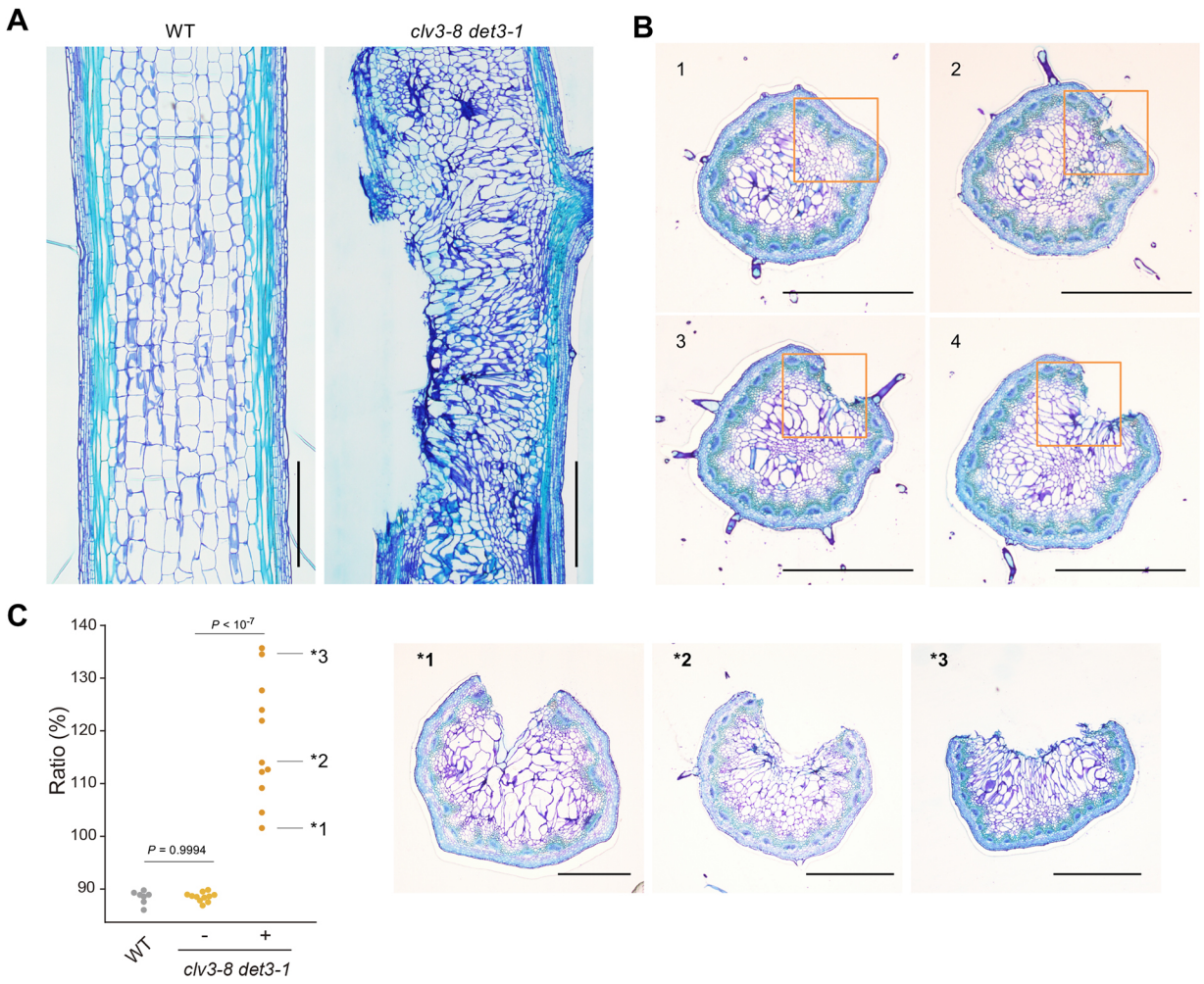

Fig. 3. Histological characterization of cracked stems. (A,B) Plants were grown for 40 days after sowing (DAS), and their stems were collected and fixed to create histological cross-sections and longitudinal sections. Histological sections were stained with Toluidine Blue. (A) Longitudinal sections of stems from WT and *clv3-8 det3-1* plants. (B) Histological cross-sections were prepared every 300 µm along cracked *clv3-8 det3-1* stems. Orange squares indicate a sequence of section from above the cracking site (panel 1) and down to the cracking site (panels 2-4). (C) Plots showing the ratios of cross-sectional area and length measurements from the stem periphery of WT and *clv3-8 det3-1* plants. Ratios were calculated by dividing the measured cross-sectional area by a theoretical cross-sectional area that is calculated from the measured stem section perimeter. *P*-values were calculated using Tukey's test. *n*=8 for WT and *n*=11 for *clv3-8 det3-1* with cracks (+) or without cracks (–). All stem cross-sectional images used for calculation were prepared from plants at 40 DAS. Representative images of *clv3-8 det3-1* cracked stems are shown (right). Scale bars: 500 µm.

real and theoretical cross-sectional areas will be greater in cracked stems than in uncracked stems if inner tissue in cracked stems has expanded. A ratio of 100% means that there is no deviation between real and theoretical cross-sectional area. The ratios calculated for cracked *clv3-8 det3-1* stems were significantly higher (121.15±14.51; mean±s.d.) than those calculated for uncracked stems (88.37±0.79; Fig. 3C). In addition, ratios calculated for stems with deeper or wider cracks were further increased, suggesting that substantial inner tissue growth occurred after the stems had cracked. Our kinetic analysis of stem development (Fig. 4) also showed that *clv3-8 det3-1* stem cross-sectional areas increased significantly, even after pith cell deformation. These findings suggest a scenario in which stem cracks unleash inner tissue growth by weakening epidermal growth constraints.

Consequently, a positive feedback loop occurs in *clv3 det3* stems: excess of growth fuels stem cracking, and cracking promotes excess of growth. Conversely, when the epidermis has not cracked yet, the growth of inner tissues is inhibited. These observations highlight the important role played by the epidermis in controlling growth and stem integrity and suggest that further analyses should focus on epidermal cells in the *clv3 det3* mutant.

Flattening of epidermal cells in *clv3-8 det3-1*

To analyze epidermal cell features, we compared four key growth stages based on *clv3-8 det3-1* inflorescence stem length. As described above, stem portions were dissected at 5 mm from the base when the main inflorescence stems reached 1, 2, 3 or 4 cm in length, and histological cross-sections were prepared (Fig. 4, Fig. S2). Strikingly, we found an intriguing relationship between epidermal cell shape and stem growth. Despite the increase in inner stem volume and in the number of pith cells, the number of epidermal cells in the stem remained constant throughout development in all genotypes (Fig. 5A,B). In addition, there were no marked changes in the cross-sectional areas of epidermal cells in any of the genotypes or growth stages examined (Fig. 5C). However, the shapes of cells varied dramatically during *clv3-8 det3-1* stem development, most notably between stems that were 1 and 3 cm in length. We quantified this morphological trait by

Development (2021) 148, dev198028. doi:10.1242/dev.198028

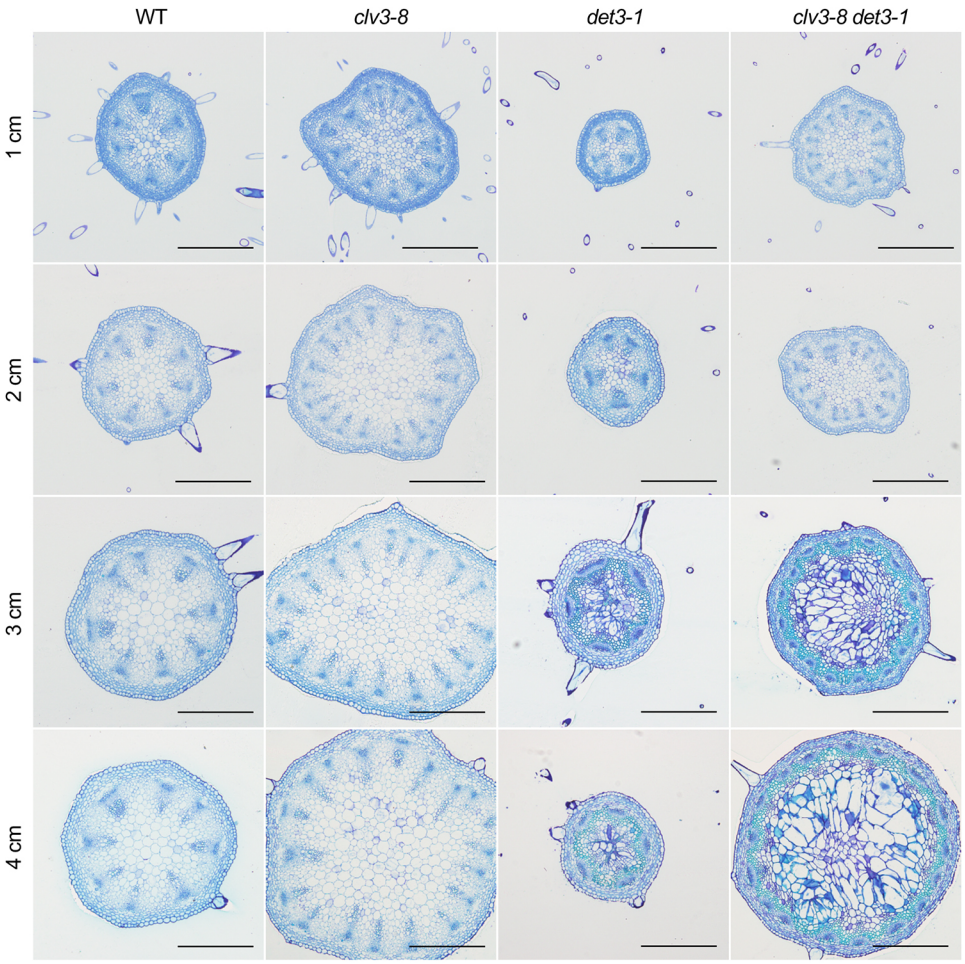

Fig. 4. Time course showing inner stem morphology at four distinct developmental stages. Histological cross-sections from WT, *clv3-8*, *det3-1* and *clv3-8 det3-1* plants showing the inner tissue organization of the flowering stem, 5 mm from its base. Stems were collected at the growth stages indicated when the flowering stems reached 1, 2, 3 and 4 cm in length. All histological cross-sections were stained with Toluidine Blue. Scale bars: 100 µm.

calculating epidermal cell aspect ratios (Fig. S4), and the results clearly indicated that epidermal cell flattening only occurred in *clv3-8 det3-1* mutants (Fig. 5D,E). These results suggest that epidermal cells respond to the increase in inner tissue volume during stem growth by halting their expansion, which produces flatter epidermal cells in *clv3 det3*. This observation is consistent with the epidermis restricting growth in the stem. To gain insight into the biophysical mechanism underlying the role of the epidermis in *clv3 det3*, we quantified its mechanical properties.

The *det3-1* stem epidermis exhibits reduced cell-wall stiffness

Anatomically, epidermal cells are distinct from inner plant cells because of their thickened cell walls. For example, in light-grown sunflower hypocotyls, epidermal cell walls are approximately 2 µm thick, whereas typical cortex cell walls are only approximately 0.2 µm thick and the walls of pith cells are even thinner (~0.1 µm; Kutschera, 1992). However, cell walls do more than simply maintain cell shape, they also play a central role in controlling growth patterns via mechanical feedback. Consequently, cell wall properties must be measured to understand whether they actively resist, via stiffening, or yield to stress (Milani et al., 2013; Sassi and Traas, 2015). In the simplest scenario, crack occurrence could reflect decreased epidermal strength. However, cracks are not always associated with weaker cell walls. For example, mature fruits crack due to cell–cell adhesion defects, and their epidermal cells exhibit increased outer wall stiffness instead (Szymańska-Chargot et al., 2016). The apparent stretching of epidermal cells in the *clv3 det3* mutant before cracks appear tends to support the former scenario. To test this hypothesis, we measured the average stiffness of epidermal cell walls in our lines.

More specifically, we measured the apparent elastic modulus of epidermal cells at the stem surface using atomic force microscopy (AFM; Milani et al., 2011, 2014). Indentations were made in single epidermal cells at two depths: <200 nm to measure wall stiffness without involving other parameters; and 0.5-1 µm to obtain more integrated, large-scale measurements of wall stiffness, albeit at depths that are slightly more sensitive to parameters such as turgor pressure and wall geometry (Milani et al., 2013). Note that neither of these indentation depths were as thick as the epidermal cell wall. We found that, at both depths, the mean values of cell wall stiffness in *clv3-8 det3-1* mutants were approximately half those of WT values (Fig. 6).

In principle, this effect may be due to *clv3-8*, *det3-1*, or a synergistic interaction involving both mutations. Therefore, we also analyzed the single mutants. This analysis demonstrated that the reduction in wall stiffness was entirely attributable to the *det3-1* mutation, consistent with previous results that showed the *det3* mutation is epistatic to *clv3* and also with the original biochemical function of DET3 in promoting etiolation (Schumacher et al., 1999). Altogether, these observations suggest that DET3 is necessary to enable the epidermis to mechanically reinforce its cell walls and constrain the growth of inner tissues.

Crack occurrence was suppressed in *pPDF1:DET3 clv3-8 det3-1* plants

To test the hypothesis that DET3 restricts growth in the epidermis, we sought to complement the *det3* mutation by generating lines that

Development (2021) 148, dev198028. doi:10.1242/dev.198028

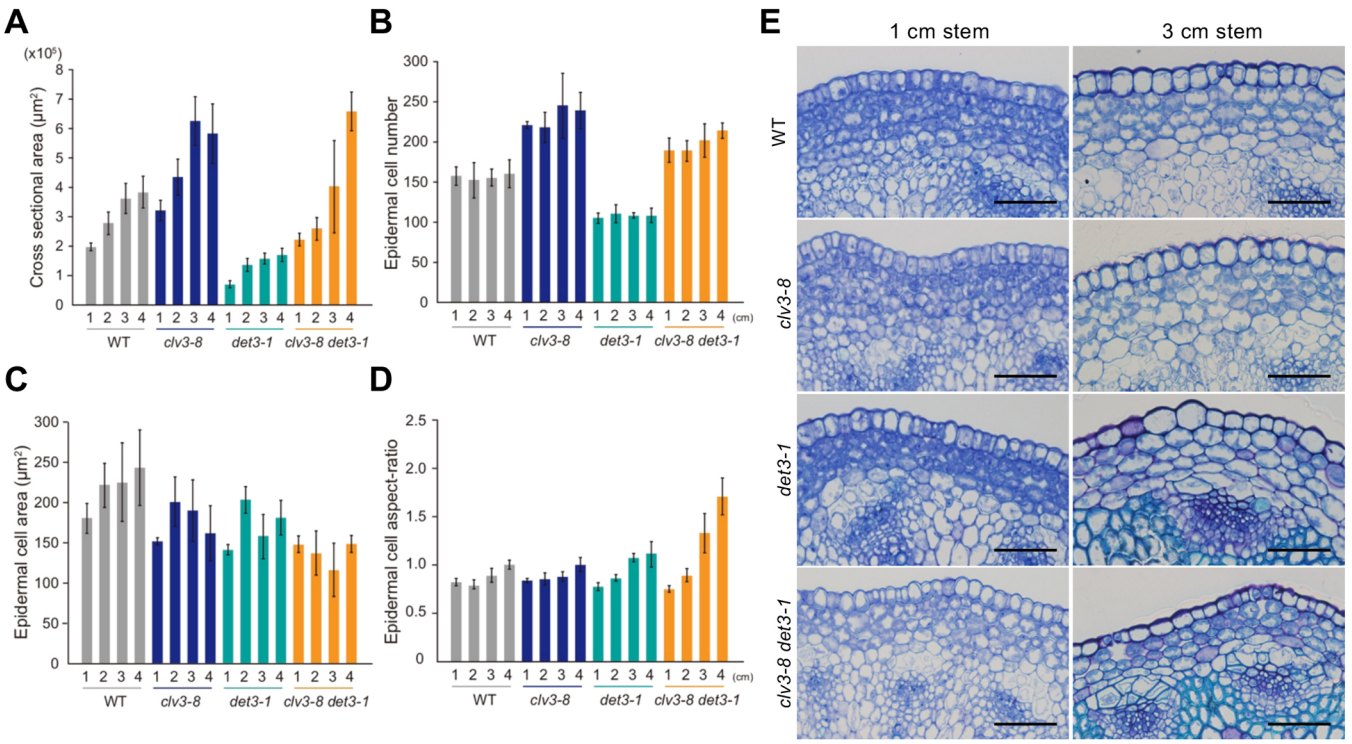

Fig. 5. Cross-sectional area of stem and epidermal cells, and characterization of epidermal cells during stem growth. (A-D) Cross-sectional area (A), number of epidermal cells (B), cross-sectional area of epidermal cells (C) and epidermal cell aspect ratio (D) (defined in this research; Fig. S4) calculated for flowering stems at four different developmental stages using the histological images shown in Fig. 4. Data are mean±s.d. (n≥5 stems). Mean values were calculated from 20 epidermal cells (C,D). (E) Representative images showing epidermal cells from 1- or 3-cm-long stems were recorded as described in Fig. 4. Scale bars: 50 µm.

expressed *DET3* specifically in the epidermis. We used the *PROTODERMAL FACTOR 1* (*PDF1*) promoter (*pPDF1:DET3 clv3-8 det3-1* hereafter), which is exclusively expressed in the epidermis (Abe et al., 2001; Kawade et al., 2013), in the *clv3-8 det3-1* background. Using these new transgenic lines, we tested whether WT DET3 activity expressed in the epidermis was sufficient to suppress the cracked stem phenotype of the *clv3 det3* mutant.

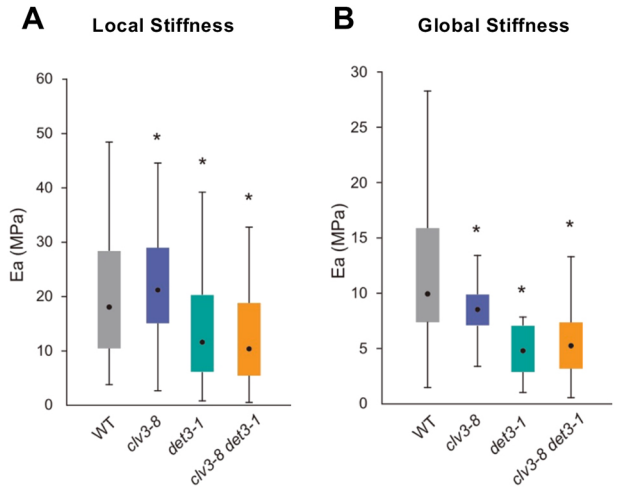

Fig. 6. Atomic force microscopy measurements of stem epidermal cell wall stiffness. (A,B) Box plots showing the apparent elastic modulus (Ea) of stem epidermal cells extracted from the atomic force microscopy force–displacement curves by local scale indentation (A; n=1059-1614 force curves from 3-5 stems) or global scale indentation (B; 688-1612 force curves from 3-5 stems). Stems were collected between 30 and 35 days after sowing. Data are mean±s.d. *P<0.01 (Steel–Dwass test).

The overall morphology of *pPDF1:DET3 clv3-8 det3-1* plants indicated that normal vegetative and stem growth were largely rescued compared with *clv3-8 det3-1* (Fig. 7A, Fig. S5). Although *pPDF1:DET3 clv3-8 det3-1* plants remained small, plant height and size were notably superior to their *clv3-8 det3-1* counterparts.

Next, we quantified the frequency of stem cracks in *pPDF1:DET3 clv3-8 det3-1* complementation lines. The frequency of stem cracking in the *pPDF1:DET3*#1 *clv3-8 det3-1* and *pPDF1:DET3*#14 *clv3-8 det3-1* transgenic lines was restored to 20% and 40% of *clv3-8 det3-1*, respectively (Fig. 7B). Furthermore, the cracks in the stems of *pPDF1:DET3 clv3-8 det3-1* plants appeared to be narrower and shallower than those observed in *clv3-8 det3-1* plants, where large regions of pith tissue were exposed (Fig. 7C; Maeda et al., 2014).

Next, we investigated the relationship between cracks and stem growth in the *pPDF1:DET3 clv3-8 det3-1* lines. Whereas the first cracks in *clv3-8 det3-1* stems occurred when plants were young or their stems were still short, cracks in *pPDF1:DET3 clv3-8 det3-1* stems occurred during later stages of growth or when the stems were longer (Fig. 7D). These results indicated that *pPDF1:DET3 clv3-8 det3-1* transgenic lines exhibited significant suppression in overall cracking frequencies and a significant delay in the appearance of the first stem crack.

Based on these observations, we prepared stem cross-sections to study the inner morphology of *pPDF1:DET3 clv3-8 det3-1* plants (Fig. 8). The cross-sectional areas of the *pPDF1:DET3 clv3-8 det3-1* lines had increased by up to 150-200% compared with *clv3-8 det3-1* plants (Fig. 8A,B). The pith cell distortion phenotype

Development (2021) 148, dev198028. doi:10.1242/dev.198028

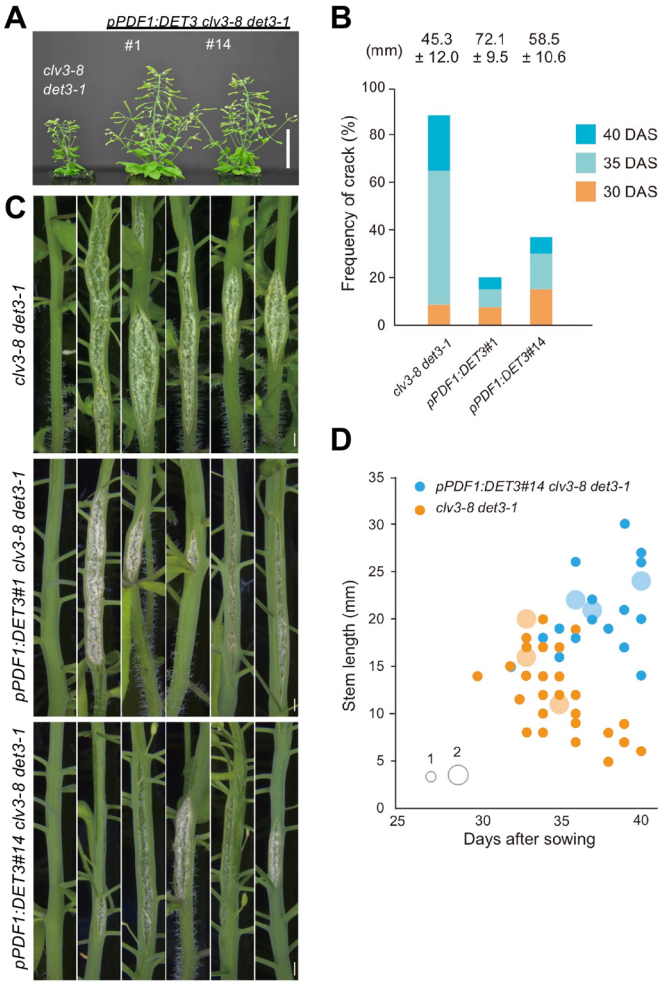

Fig. 7. Tissue-specific complementation using the *DET3* gene reduced stem cracking in *clv3-8 det3-1*. (A) Overall morphology of *pPDF1:DET3 clv3-8 det3-1* lines at 40 days after sowing (DAS) compared with *clv3-8 det3-1*. (B) Frequency of stem cracking in two independent *pPDF1:DET3 clv3-8 det3-1* transgenic lines. Cracks occurring in the main stem were monitored at 30, 35 and 40 DAS. The mean stem length at 40 DAS is indicated (n=40; data are mean±s.d.). (C) Cracked stems in *clv3-8 det3-1*, *pPDF1:DET3#1 clv3-8 det3-1* and *pPDF1:DET3#14 clv3-8 det3-1* plants. (D) The relationship between flowering stem length and the timing of cracks occurring in *clv3-8 det3-1* and *pPDF1:DET3#14 clv3-8 det3-1* plants. Flowering stem length and crack occurrence between 25 and 40 DAS. The time (DAS) when the first crack was identified (x-axis) and the flowering stem length (y-axis) were plotted. The spot size indicates the number of plants showing cracks at the same time point (n=32 for *clv3-8 det3-1*; n=22 for *pPDF1:DET3#14 clv3-8 det3-1*). Scale bars: 3 cm (A); 1 mm (C).

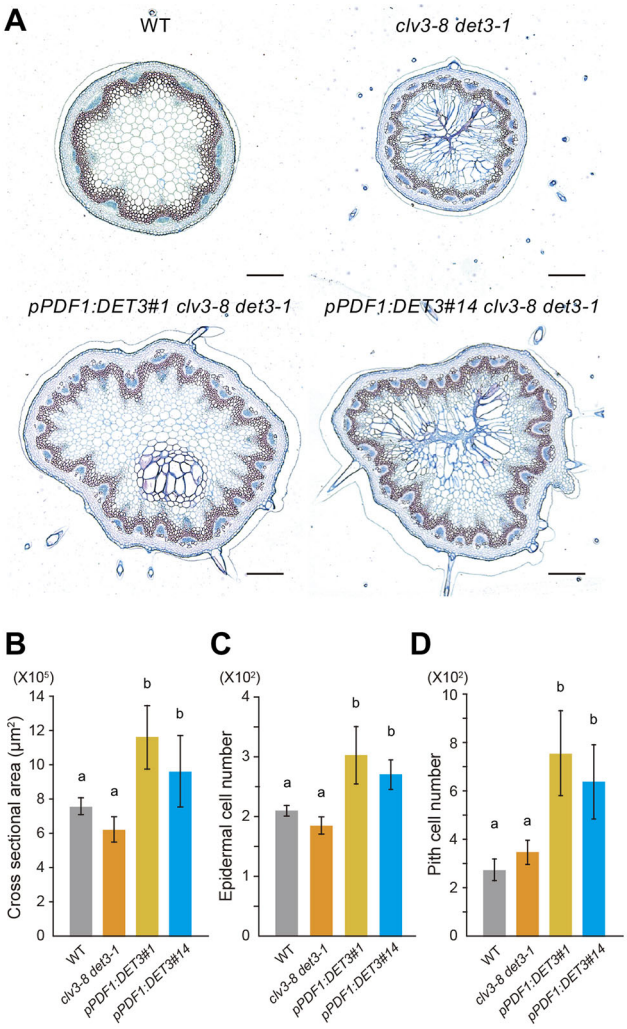

Fig. 8. Impact of epidermis-specific expression of the *DET3* gene on overall stem phenotype and inner tissue morphology in the *clv3-8 det3-1* background. (A) Histological cross-sections showing inner tissue organization of inflorescence stems collected at 40 days after sowing. Sections were stained with Safranin and Astra Blue. (B-D) The cross-sectional areas and cellular parameters of flowering stems were determined from histological images (n=6 stems). Data are mean±s.d.; lower case letters are used to label means, such that bars bearing different letters are statistically different from one another with a minimum P-value of <0.05 (Tukey's test). Scale bars: 100 µm.

remained in the *pPDF1:DET3 clv3-8 det3-1* lines but was less marked than in *clv3-8 det3-1* plants, and it was restricted to small clusters of cells (Fig. 8A). Importantly, the number of epidermal and pith cells had increased significantly, correlating with the increase in cross-sectional area (Fig. 8C,D). Taken together, these findings strongly suggest that epidermis-targeted expression of DET3 effectively restores the ability of the epidermis to resist mechanical stress from the inner stem tissue and that the epidermis acts as a load-bearing layer to maintain stem integrity.

DISCUSSION

Based on our results, we can now provide a scenario explaining the appearance of cracks in *clv3-8 det3-1* stems. The *det3-1* mutation leads to weaker walls, probably owing to defects in exocytosis and cell wall synthesis. The *clv3-8* mutation generates a large pool of growing cells, amplifying the mechanical conflict between inner cells and the epidermis. When combined, the *det3* and *clv3* mutations increase tension in the epidermis. The *det3-1* mutation also weakens the walls of cells in the epidermis, and these cells become stretched to the point of mechanical failure, leading to cracks. In inner tissues, lignified pith cells appear in the *det3-1* and *clv3-8 det3-1* mutants because weakening of the cell walls triggers the wall integrity pathway (Hématy et al., 2007). Our results also suggest that the cracks relieve the constraints on growth imposed by the epidermis and allow inner cells to expand further, in a positive feedback loop. Because the expression of DET3 in the epidermis is sufficient to rescue most of these defects, our results are consistent with the epidermal growth theory and suggest that DET3 plays a key role in maintaining stem integrity.

Development (2021) 148, dev198028. doi:10.1242/dev.198028

Our results are consistent with a simple scenario in which the epidermis constrains growth. This hypothesis was developed to explain the results of peeling experiments (Baskin and Jensen, 2013; Peters and Tomos, 2000) and is compatible with Hofmeister's tissue tension theory (Hofmeister, 1859). Here, we not only confirm this biophysical view of the stem but also provide evidence that such mechanical balance requires the regulation of cell number (CLV3) and wall stiffness (DET3). The spontaneous expansion of pith tissue cells after stem cracking (Fig. 3C) illustrates this point. Our findings show that a fundamental process in stem development can resist mechanical conflict between the inner tissues and the epidermis (Galletti et al., 2016). However, there is a threshold beyond which the tissue becomes unable to resist.

The stretched and flattened epidermal cells found in the *clv3 det3* mutant are particularly interesting because cell wall defects often lead to responses that rescue the original defect and may even overcompensate for it. This may explain the lignification that occurs following wall weakening. The *det3-1* mutant has weak walls and the cells break when the level of tension becomes too great. However, because this does not occur in the epidermis, DET3 may play a different role in the wall integrity pathway there. However, lignification is triggered in other tissues in the *det3-1* mutant, as it is in the *theseus1* mutant, which is deficient in a protein involved in sensing cell wall integrity. Importantly, even if the cell wall integrity pathway is triggered, it may be unable to produce a response capable of withstanding the formidable mechanical stress built up in the inner tissue. Here, the positive feedback that stimulates growth following crack emergence may further explain why stems cannot withstand the excessive mechanical stress from inner tissues in *clv3-8 det3-1* because when a local defect occurs in the epidermis, the feedback loop would rapidly amplify any damage already present.

Because the biochemical role of DET3 is primarily related to vesicle trafficking, it is unlikely to affect the mechanical anisotropy of cell walls, at least directly. For example, the export of cellulose synthase to the plasma membrane may be impaired, but any defects in cellulose microfibril orientation would rather be the consequence of defective wall remodeling. Yet, DET3 may still have a role of directional growth, notably assuming that exocytosis can be polarized and that walls can be mechanically heterogeneous. Such mechanical polarities have been observed in hypocotyls (Peaucelle et al., 2015) and cotyledons (Majda et al., 2017). The presence of longitudinal cracks in *clv3 det3* is consistent with a failure to resist tensile stress magnitude and/or direction. Whether DET3 function also contributes to anisotropic wall reinforcement remains to be explored.

The *clv3 det3* mutant demonstrates that epidermal cells weaken and become flatter when the growth rate of inner tissues becomes too high. Coordinating the necessary responses requires a perception mechanism, which may involve mechanotransduction. This echoes the concept of proprioception, the ability of an organism to sense its own shape and growth (Hamant and Moulia, 2016), and the presence of cracks may be viewed as a defect in that pathway too. The role of DET3 in proprioception may be an interesting avenue for future research. Our histological studies have provided new insight into why plant stems may crack during development. However, further molecular analyses are needed to unravel the role of mechanoperception, identify signaling components and understand the transduction mechanisms that are important in plant stem development. Finally, our findings may be relevant for biomechanical applications wherein active materials, amenable to auto-repair or self-reinforcement in response to stress, may be used constructively.

MATERIALS AND METHODS

Plant materials and growth conditions

The WT *A. thaliana* ecotype used in this study was Columbia-0 (Col-0). All other mutants were in the Col-0 background, except *clv1-4* and *clv2-1*, which were both in the Landsberg *erecta* (L*er*) background. The *clv1-4*, *clv2-1*, *clv3-8* and *det3-1* single mutants, and all corresponding double mutants with *det3-1*, have been described previously (Maeda et al., 2014). The *clv3-101* allele is a novel allele of *clv3* that we isolated in the *det3-1* background, as described previously (Ferjani et al., 2015; Maeda et al., 2014). *pPDF1:DET3* lines were generated for this study, as described below. Seeds were sown on rockwool (Nitto Boseki), watered daily with 0.5 g l^{-1} Hyponex solution (Hyponex) and grown at 22°C under a 16 h light/8 h dark cycle with white light fluorescent lamps at approximately 50 µmol m^{-2} s^{-1}, as described previously (Ferjani et al., 2013).

Morphological observations

Images showing overall plant phenotypes were recorded using a Nikon D5000 NIKKOR lens and AF-S Micro NIKKOR 60-mm digital camera (Nikon). Images showing cracked stems were recorded using a Leica M165 FC stereoscopic microscope connected to a CCD camera (DFC 7000T; Leica Microsystems). The appearance of cracks was monitored with the naked eye and by using an ordinary loupe.

Preparation and observation of histological sections

For the histological cross-sections and longitudinal sections, portions of the first internode from the main flowering stem were dissected and fixed overnight in formalin–acetic acid–alcohol (4% formalin, 5% acetic acid, 50% ethanol) at room temperature. Then, samples were dehydrated using a graded series of ethanol washes [50%, 60%, 70%, 80%, 90% and 95% (v/v); 30 min each] and stored overnight in 99.5% (v/v) ethanol at room temperature. Next, fixed specimens were embedded in Technovit resin (Kulzer), in accordance with the manufacturer's instructions, and sectioned using a microtome (RM2125 RTS; Leica Microsystems). Sections were stained with Toluidine Blue or Safranin or double stained with Astra Blue–Safranin and photographed under a microscope (Leica DM6 B) connected to a CCD camera (DFC 7000T; Leica Microsystems). Images were analyzed using ImageJ software (LOCI; University of Wisconsin, Madison, WI, USA). Statistical analyses were performed using R software (ver. 3.6.1; R Development Core Team).

AFM

A Catalyst Bioscope (Bruker) mounted under a MacroFluo optical epifluorescence macroscope (Leica Microsystems) was used for the AFM indentation experiments. A 2× Plano objective was used to observe the apices (Leica Microsystems). To record surface topology and stiffness modulus maps, we used PeakForce QNM AFM mode (Bruker/Veeco), a NanoScope V controller and NanoScope software (ver. 8.1; Bruker). All quantitative measurements were recorded using SD-Sphere-NCH 0.8-µm-diameter spherical probes (NANOSENSORS). The spring constant of cantilevers (42 N m^{-1}) was measured using the thermal tuning method (Hutter and Bechhoefer, 1993; Lévy and Maaloum, 2009). All measurements were recorded under water at room temperature, and the standard cantilever holder for operating in liquid environments was used. The 30 mm Petri dishes containing each sample (~2-3 cm of stem) were placed on an XY stage in a customized sample holder. Then, the AFM head was mounted on the stage and positioned with the cantilever over relatively flat areas that were free from trichomes. To extract elastic moduli from the force–indentation retract curves, we used the Hertz model, which applies to the adhesive contact between two elastic, thick isotropic solids (Derjaguin et al., 1975). Images were obtained using the following parameters: scan size, 50 µm; force, 423 nN. For the point and shoot mode, the following parameters were used: size, 50×15 µm, 20×20 points; trig threshold, 247 nm; ramp size, 4 µm.

Generation of transgenic plants

The full-length cDNA of the *DET3* gene coding region was amplified by PCR using a pair of oligonucleotides: DET3-B1-FW 5′-GGGGACAAGTTT-

GTACAAAAAAGCAGGCTATGACTTCGAGATATTGGGTG-3′ and D-ET3-B2-RV 5′-GGGGACCACTTTGTACAAGAAAGCTGGGTTTAAG-CAAGGTTGATAGTGAAG-3′.

The amplified fragments were fused into pDONR201 using the BP recombination system (Invitrogen). The DNA sequences of all clones were confirmed by sequencing. The LR reaction was used to convert the resulting vector (pDONR201–DET3), pENTP4P1R–pPDF1 (Kawade et al., 2013) and the R4 gateway binary vector R4pGWB501 (Nakagawa et al., 2008) into R4pGWB501–pPDF1–DET3. The final constructs were used to transform WT plants via the floral dip method (Clough and Bent, 1998). Several independent homozygous T_3 lines expressing the *DET3* gene driven by *PDF1* promoters from a single T-DNA insertion locus were identified in the WT background. Representative lines (*pPDF1:DET3*#1 and *pPDF1:DET3*#14) were then crossed to *clv3-8 det3-1* to obtain the final complementation lines, and these were used in the study.

Acknowledgements
We thank T. Nakagawa (Shimane University) for providing the R4pGWB501 binary vector, and K. Kawade (National Institute for Basic Biology) for providing the *pENTP4P1R-pPDF1* vector.

Competing interests
The authors declare no competing or financial interests.

Author contributions
Conceptualization: M.A., M.O., A.F.; Methodology: M.O., S.G., P.M., G.H., O.H., A.F.; Validation: M.A., M.O., P.M., A.F.; Formal analysis: M.A., M.O., S.G., P.M., G.R., A.F.; Resources: A.F.; Data curation: M.A., M.O., S.G., P.M., G.R., A.F.; Writing - original draft: M.A., A.F.; Writing - review & editing: O.H., S.S., H.T., A.F.; Supervision: G.H., O.H., S.S., H.T., A.F.; Project administration: A.F.; Funding acquisition: O.H., S.S., H.T., A.F.

Funding
This work was supported by the Ministry of Education, Culture, Sports, Science and Technology of Japan Grant-in-Aid for Encouragement of Young Scientists (B) (21770036 to A.F.), Grant-in-Aid for Scientific Research (B) (16H04803 to A.F.), Grant-in-Aid for Scientific Research on Innovative Areas (25113002 to H.T. and A.F.; 18H05487 to S.S. and A.F.; 19H05672 to H.T.) and the European Research Council (ERC-2013-CoG-615739 'MechanoDevo'). M.A. is a recipient of Japan Society for the Promotion of Science Overseas Research Fellowships.

Supplementary information
Supplementary information available online at
https://dev.biologists.org/lookup/doi/10.1242/dev.198028.supplemental

References
Abe, M., Takahashi, T. and Komeda, Y. (2001). Identification of a cis–regulatory element for L1 layer–specific gene expression, which is targeted by an L1–specific homeodomain protein. *Plant J.* **26**, 487-494. doi:10.1046/j.1365-313x.2001.01047.x

Baskin, T. I. and Jensen, O. E. (2013). On the role of stress anisotropy in the growth of stems. *J. Exp. Bot.* **64**, 4697-4707. doi:10.1093/jxb/ert176

Betsuyaku, S., Sawa, S. and Yamada, M. (2011). The function of the CLE peptides in plant development and plant–microbe interactions. *Arabidopsis Book* **9**, e0149. doi:10.1199/tab.0149

Caño-Delgado, A. I., Metzlaff, K. and Bevan, M. W. (2000). The *eli1* mutation reveals a link between cell expansion and secondary cell wall formation in *Arabidopsis thaliana*. *Development* **127**, 3395-3405.

Caño-Delgado, A., Penfield, S., Smith, C., Catley, M. and Bevan, M. (2003). Reduced cellulose synthesis invokes lignification and defense responses in *Arabidopsis thaliana*. *Plant J.* **34**, 351-362. doi:10.1046/j.1365-313X.2003.01729.x

Clough, S. J. and Bent, A. F. (1998). Floral dip: a simplified method for *Agrobacterium*-mediated transformation of *Arabidopsis thaliana*. *Plant J.* **16**, 735-743. doi:10.1046/j.1365-313x.1998.00343.x

Derjaguin, B. V., Muller, V. M. and Toporov, Y. P. (1975). Effect of contact deformations on the adhesion of particles. *J. Colloid Interface Sci.* **53**, 314-326. doi:10.1016/0021-9797(75)90018-1

Ferjani, A., Ishikawa, K., Asaoka, M., Ishida, M., Horiguchi, G., Maeshima, M. and Tsukaya, H. (2013). Enhanced cell expansion in a *KRP2* overexpressor is mediated by increased V-ATPase activity. *Plant Cell Physiol.* **54**, 1989-1998. doi:10.1093/pcp/pct138

Ferjani, A., Hanai, K., Gunji, S., Maeda, S., Sawa, S. and Tsukaya, H. (2015). Balanced cell proliferation and expansion is essential for flowering stem growth control. *Plant Signal. Behav.* **10**, e992755. doi:10.4161/15592324.2014.992755

Finet, C. and Jaillais, Y. (2012). Auxology: when auxin meets plant evo-devo. *Dev. Biol.* **369**, 19-31. doi:10.1016/j.ydbio.2012.05.039

Fukao, Y., Ferjani, A., Tomioka, R., Nagasaki, N., Kurata, R., Nishimori, Y., Fujiwara, M. and Maeshima, M. (2011). iTRAQ analysis reveals mechanisms of growth defects due to excess zinc in Arabidopsis. *Plant Physiol.* **155**, 1893-1907. doi:10.1104/pp.110.169730

Galletti, R., Verger, S., Hamant, O. and Ingram, G. C. (2016). Developing a 'thick skin': a paradoxical role for mechanical tension in maintaining epidermal integrity? *Development* **143**, 3249-3258. doi:10.1242/dev.132837

Gruel, J., Landrein, B., Tarr, P., Schuster, C., Refahi, Y., Sampathkumar, A., Hamant, O., Meyerowitz, E. M. and Jönsson, H. (2016). An epidermis-driven mechanism positions and scales stem cell niches in plants. *Sci. Adv.* **2**, e1500989. doi:10.1126/sciadv.1500989

Hamant, O. and Haswell, E. S. (2017). Life behind the wall: sensing mechanical cues in plants. *BMC Biol.* **15**, 59. doi:10.1186/s12915-017-0403-5

Hamant, O. and Moulia, B. (2016). How do plants read their own shapes? *New Phytol.* **212**, 333-337. doi:10.1111/nph.14143

Hejnowicz, Z. and Sievers, A. (1996). Tissue stresses in organs of herbaceous plants III. Elastic properties of the tissues of sunflower hypocotyl and origin of tissue stresses. *J. Exp. Bot.* **47**, 519-528. doi:10.1093/jxb/47.4.519

Hématy, K., Sado, P.-E., Van Tuinen, A., Rochange, S., Desnos, T., Balzergue, S., Pelletier, S., Renou, J.-P. and Höfte, H. (2007). A receptor-like kinase mediates the response of *Arabidopsis* cells to the inhibition of cellulose synthesis. *Curr. Biol.* **17**, 922-931. doi:10.1016/j.cub.2007.05.018

Hofmeister, W. (1859). Über die Beugungen saftreicher Pflanzenteile nach Erschütterung. *Ber Verh Ges Wiss Leipz*. 175-204.

Hutter, J. L. and Bechhoefer, J. (1993). Calibration of atomic-force microscope tips. *Rev. Sci. Instrum.* **64**, 1868-1873. doi:10.1063/1.1143970

Kawade, K., Horiguchi, G., Usami, T., Hirai, M. Y. and Tsukaya, H. (2013). ANGUSTIFOLIA3 signaling coordinates proliferation between clonally distinct cells in leaves. *Curr. Biol.* **23**, 788-792. doi:10.1016/j.cub.2013.03.044

Kinoshita, A., Betsuyaku, S., Osakabe, Y., Mizuno, S., Nagawa, S., Stahl, Y., Simon, R., Yamaguchi-Shinozaki, K., Fukuda, H. and Sawa, S. (2010). RPK2 is an essential receptor–like kinase that transmits the CLV3 signal in *Arabidopsis*. *Development* **137**, 3911-3920. doi:10.1242/dev.048199

Kutschera, U. (1992). The role of the epidermis in the control of elongation growth in stems and coleoptiles. *Bot. Acta.* **105**, 246-252. doi:10.1111/j.1438-8677.1992.tb00294.x

Kutschera, U. and Niklas, K. J. (2007). The epidermal-growth-control theory of stem elongation: an old and a new perspective. *J. Plant Physiol.* **164**, 1395-1409. doi:10.1016/j.jplph.2007.08.002

Laufs, P., Grandjean, O., Jonak, C., Kiêu, K. and Traas, J. (1998). Cellular parameters of the shoot apical meristem in *Arabidopsis*. *Plant Cell* **10**, 1375-1390. doi:10.2307/3870647

Lévy, R. and Maaloum, M. (2009). Measuring the spring constant of atomic force microscope cantilevers: thermal fluctuations and other methods. *Nanotechnology* **13**, 33-37. doi:10.1088/0957-4484/13/1/307

Luo, Y., Scholl, S., Doering, A., Zhang, Y., Irani, N. G., Di Rubbo, S., Neumetzler, L., Krishnamoorthy, P., Van Houtte, I., Mylle, E. et al. (2015). V-ATPase activity in the TGN/EE is required for exocytosis and recycling in Arabidopsis. *Nat. Plants* **1**, 15094. doi:10.1038/nplants.2015.94

Maeda, S., Gunji, S., Hanai, K., Hirano, T., Kazama, Y., Ohbayashi, I., Abe, T., Sawa, S., Tsukaya, H. and Ferjani, A. (2014). The conflict between cell proliferation and expansion primarily affects stem organogenesis in *Arabidopsis*. *Plant Cell Physiol.* **55**, 1994-2007. doi:10.1093/pcp/pcu131

Majda, M., Grones, P., Sintorn, I. M., Vain, T., Milani, P., Krupinski, P., Zagórska-Marek, B., Viotti, C., Jönsson, H., Mellerowicz, E. J. et al. (2017). Mechanochemical polarization of contiguous cell walls shapes plant pavement cells. *Dev. Cell* **43**, 290-304.e4. doi:10.1016/j.devcel.2017.10.017

Milani, P., Gholamirad, M., Traas, J., Arnéodo, A., Boudaoud, A., Argoul, F. and Hamant, O. (2011). *In vivo* analysis of local wall stiffness at the shoot apical meristem in Arabidopsis using atomic force microscopy. *Plant J.* **67**, 1116-1123. doi:10.1111/j.1365-313X.2011.04649.x

Milani, P., Braybrook, S. A. and Boudaoud, A. (2013). Shrinking the hammer: micromechanical approaches to morphogenesis. *J. Exp. Bot.* **64**, 4651-4662. doi:10.1093/jxb/ert169

Milani, P., Mirabet, V., Cellier, C., Rozier, F., Hamant, O., Das, P. and Boudaoud, A. (2014). Matching patterns of gene expression to mechanical stiffness at cell resolution through quantitative tandem epifluorescence and nanoindentation. *Plant Physiol.* **165**, 1399-1408. doi:10.1104/pp.114.237115

Miwa, H., Betsuyaku, S., Iwamoto, K., Kinoshita, A., Fukuda, H. and Sawa, S. (2008). The receptor-like kinase SOL2 mediates CLE signaling in Arabidopsis. *Plant Cell Physiol.* **49**, 1752-1757. doi:10.1093/pcp/pcn148

Miwa, H., Kinoshita, A., Fukuda, H. and Sawa, S. (2009). Plant meristems: CLAVATA3/ESR-related signaling in the shoot apical meristem and the root apical meristem. *J. Plant Res.* **122**, 31-39. doi:10.1007/s10265-008-0207-3

Müller, R., Bleckmann, A. and Simon, R. (2008). The receptor kinase CORYNE of *Arabidopsis* transmits the stem cell-limiting signal CLAVATA3 independently of CLAVATA1. *Plant Cell* **20**, 934-946. doi:10.1105/tpc.107.057547

Nakagawa, T., Nakamura, S., Tanaka, K., Kawamukai, M., Suzuki, T., Nakamura, K., Kimura, T. and Ishiguro, S. (2008). Development of R4 gateway binary vectors (R4pGWB) enabling high-throughput promoter swapping for plant research. *Biosci. Biotechnol. Biochem.* **72**, 624-629. doi:10.1271/bbb.70678

Newman, L. J., Perazza, D. E., Juda, L. and Campbell, M. M. (2004). Involvement of the R2R3–MYB, AtMYB61, in the ectopic lignification and dark–photomorphogenic components of the *det3* mutant phenotype. *Plant J.* **37**, 239-250. doi:10.1046/j.1365-313X.2003.01953.x

Niklas, K. J. and Paolillo, D. J. (1997). The role of the epidermis as a stiffening agent in *Tulipa* (Liliaceae) stems. *Am. J. Bot.* **84**, 735-744. doi:10.2307/2445809

Padmanaban, S., Lin, X., Perera, I., Kawamura, Y. and Sze, H. (2004). Differential expression of vacuolar H^+-ATPase subunit c genes in tissues active in membrane trafficking and their roles in plant growth as revealed by RNAi. *Plant Physiol.* **134**, 1514-1526. doi:10.1104/pp.103.034025

Peaucelle, A., Wightman, R. and Höfte, H. (2015). The control of growth symmetry breaking in the Arabidopsis hypocotyl. *Curr. Biol.* **25**, 1746-1752. doi:10.1016/j.cub.2015.05.022

Peters, W. S. and Tomos, A. D. (2000). The mechanical state of “inner tissues” in the growing zone of sunflower hypocotyls and the regulation of its growth rate following excision. *Plant Physiol.* **123**, 605-612. doi:10.1104/pp.123.2.605

Reddy, G. V. and Meyerowitz, E. M. (2005). Stem-cell homeostasis and growth dynamics can be uncoupled in the *Arabidopsis* shoot apex. *Science* **310**, 663-667. doi:10.1126/science.1116261

Rogers, L. A., Dubos, C., Surman, C., Willment, J., Cullis, I. F., Mansfield, S. D. and Campbell, M. M. (2005). Comparison of lignin deposition in three ectopic lignification mutants. *New Phytol.* **168**, 123-140. doi:10.1111/j.1469-8137.2005.01496.x

Sassi, M. and Traas, J. (2015). When biochemistry meets mechanics: a systems view of growth control in plants. *Curr. Opin. Plant Biol.* **28**, 137-143. doi:10.1016/j.pbi.2015.10.005

Savaldi-Goldstein, S., Peto, C. and Chory, J. (2007). The epidermis both drives and restricts plant shoot growth. *Nature* **446**, 199-202. doi:10.1038/nature05618

Schumacher, K., Vafeados, D., McCarthy, M., Sze, H., Wilkins, T. and Chory, J. (1999). The *Arabidopsis det3* mutant reveals a central role for the vacuolar H^+–ATPase in plant growth and development. *Genes Dev.* **13**, 3259-3270. doi:10.1101/gad.13.24.3259

Skopelitis, D. S., Benkovics, A. H., Husbands, A. Y. and Timmermans, M. C. P. (2017). Boundary formation through a direct threshold-based readout of mobile small RNA gradients. *Dev. Cell* **43**, 265-273.e6. doi:10.1016/j.devcel.2017.10.003

Szymańska-Chargot, M., Chylińska, M., Pieczywek, P. M., Rösch, P., Schmitt, M., Popp, J. and Zdunek, A. (2016). Raman imaging of changes in the polysaccharides distribution in the cell wall during apple fruit development and senescence. *Planta* **243**, 935-945. doi:10.1007/s00425-015-2456-4

Vaseva, I. I., Qudeimat, E., Potuschak, T., Du, Y., Genschik, P., Vandenbussche, F. and Van Der Straeten, D. (2018). The plant hormone ethylene restricts *Arabidopsis* growth via the epidermis. *Proc. Natl. Acad. Sci. USA* **115**, E4130-E4139. doi:10.1073/pnas.1717649115

Verger, S., Long, Y., Boudaoud, A. and Hamant, O. (2018). A tension-adhesion feedback loop in plant epidermis. *eLife* **7**, e34460. doi:10.7554/eLife.34460

Vermeer, J. E. M., von Wangenheim, D., Barberon, M., Lee, Y., Stelzer, E. H. K., Maizel, A. and Geldner, N. (2014). A spatial accommodation by neighboring cells is required for organ initiation in *Arabidopsis*. *Science* **343**, 178-183. doi:10.1126/science.1245871

Zhao, F., Du, F., Oliveri, H., Zhou, L., Ali, O., Chen, W., Feng, S., Wang, Q., Lü, S., Long, M. et al. (2020). Microtubule-mediated wall anisotropy contributes to leaf blade flattening. *Curr. Biol.* **30**, 3972-3985.e8. doi:10.1016/j.cub.2020.07.076